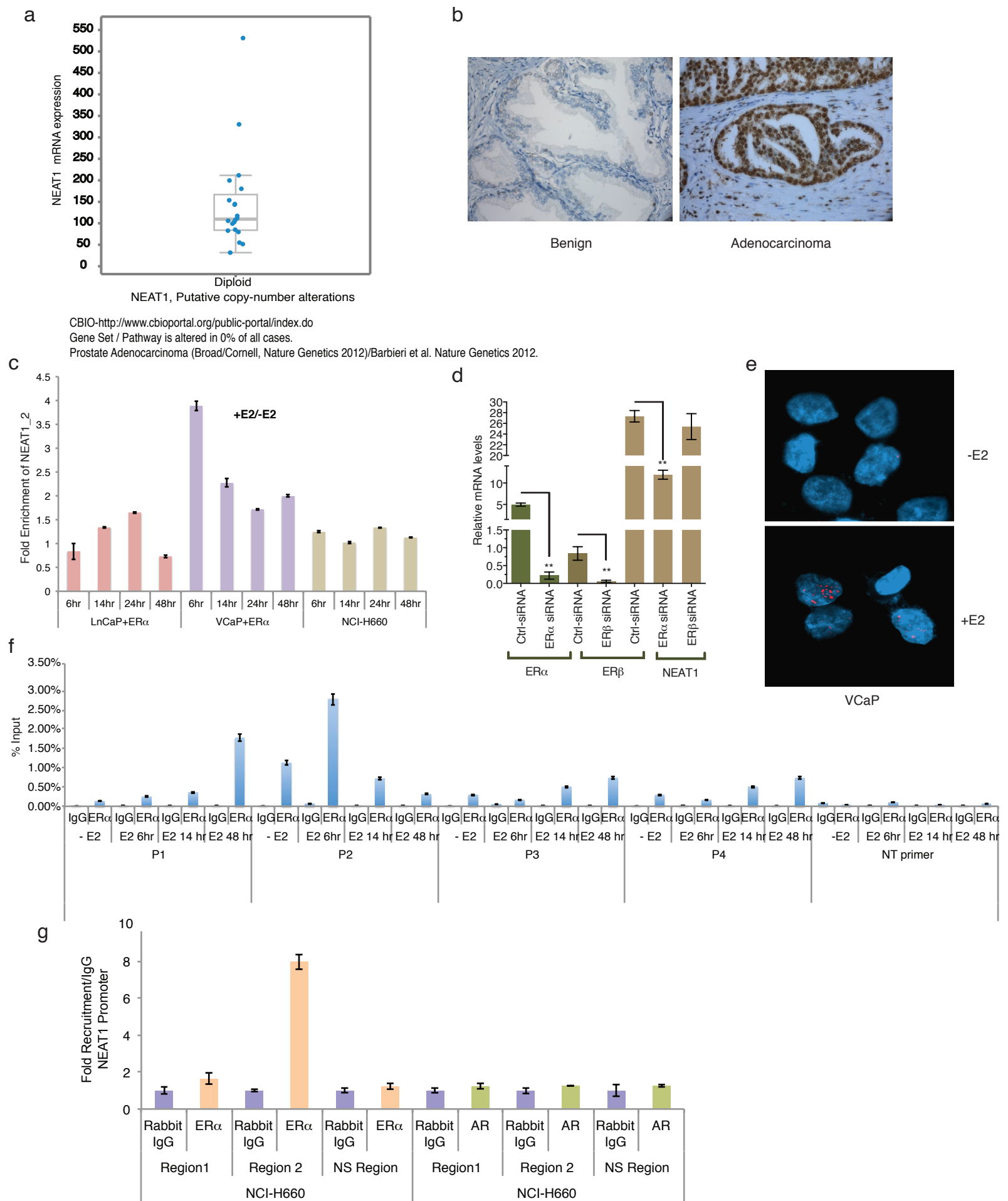


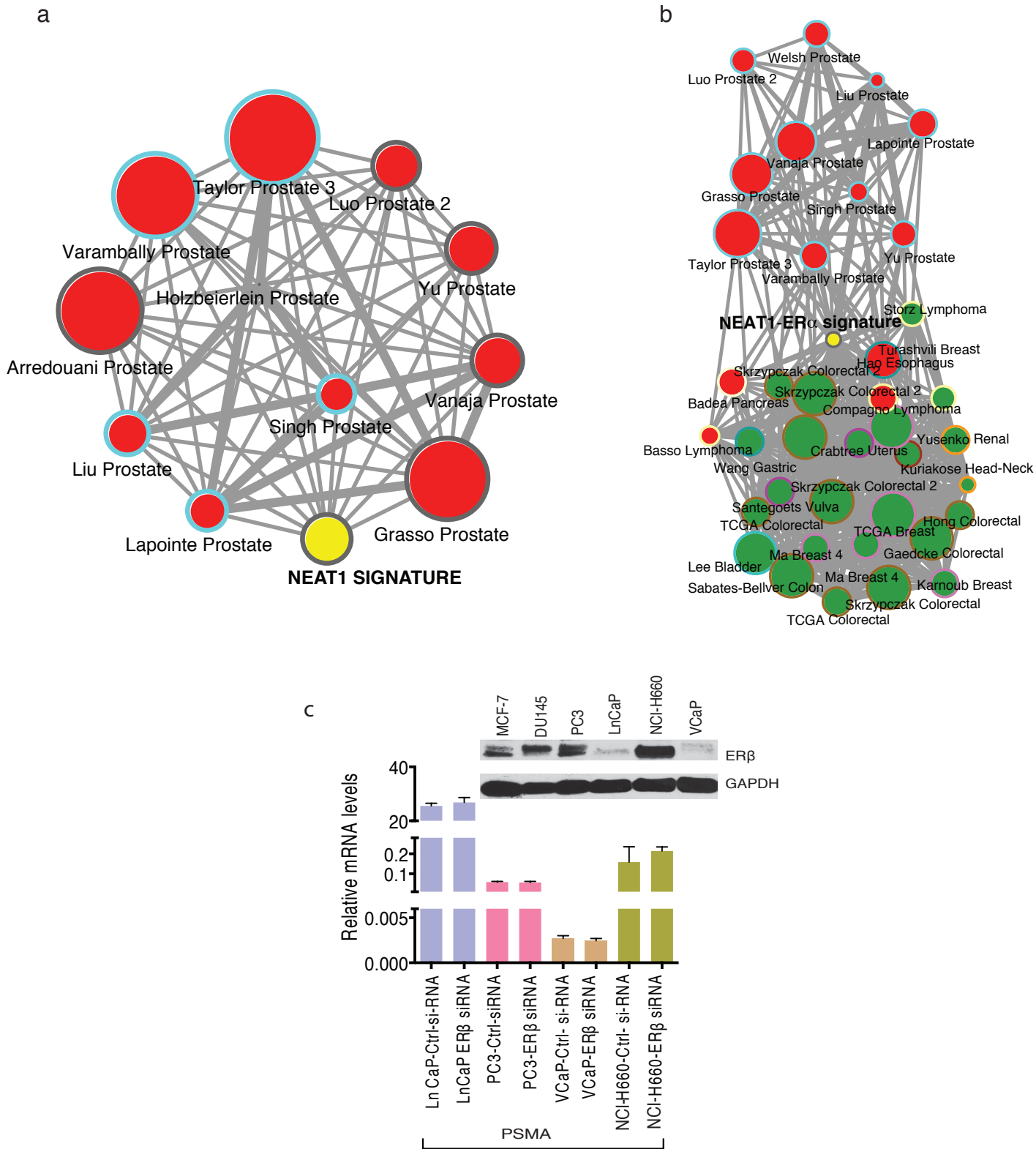
Supplementary Fig. 1

(a) ER $\alpha$  protein expression and localization was evaluated in benign, high grade prostate intraepithelial neoplasia (HGPIN), prostate adenocarcinoma (PCa) and in neuroendocrine prostate cancer (NEPC) cases using immunohistochemistry (IHC) on tissue microarrays. Representative ER $\alpha$  staining in benign prostate, HGPIN and adenocarcinoma is shown on cores; benign prostate (asterisk), HGPIN (arrow head) and PCa (arrow). Focal nuclear staining of ER $\alpha$  was detected in tumor cells and basal cells of adjacent HGPIN (left panel). Focal cytoplasmic staining of ER $\alpha$  was observed in PCa while adjacent benign zones are negative (right panel). (b) ER $\alpha$  expression by western blotting in cytoplasmic and nuclear extracts of MCF7, RWPE1, LnCaP, VCaP and NCI-H660 cells. (c) (left) ER $\alpha$  expression in VCaP control and VCaP ER $\alpha$  expressing cells. (Right) ER $\alpha$  and AR protein levels in VCaP ER $\alpha$  control siRNA and AR siRNA expressing cells (d) Venn diagram demonstrates overlap between ER $\alpha$  peak distributions in VCaP prostate cancer cell line and MCF7 breast cancer cells induced by estrogen. (e) Distribution of ER $\alpha$  binding based on the union of VCaP ER $\alpha$  and NCI-H660 cells ER $\alpha$  binding sites. (f) Expression of ER $\alpha$  regulated lncRNA in VCaP and VCaP ER $\alpha$  cells with and without E2 treatment; Results are expressed as the means $\pm$ s.d. of three independent experiments. Student's *t*-test was performed for comparisons (relative mRNA levels) between VCaP and VCaP ER $\alpha$  (-E2 condition) and VCaP and VCaP ER $\alpha$  (+E2) conditions.



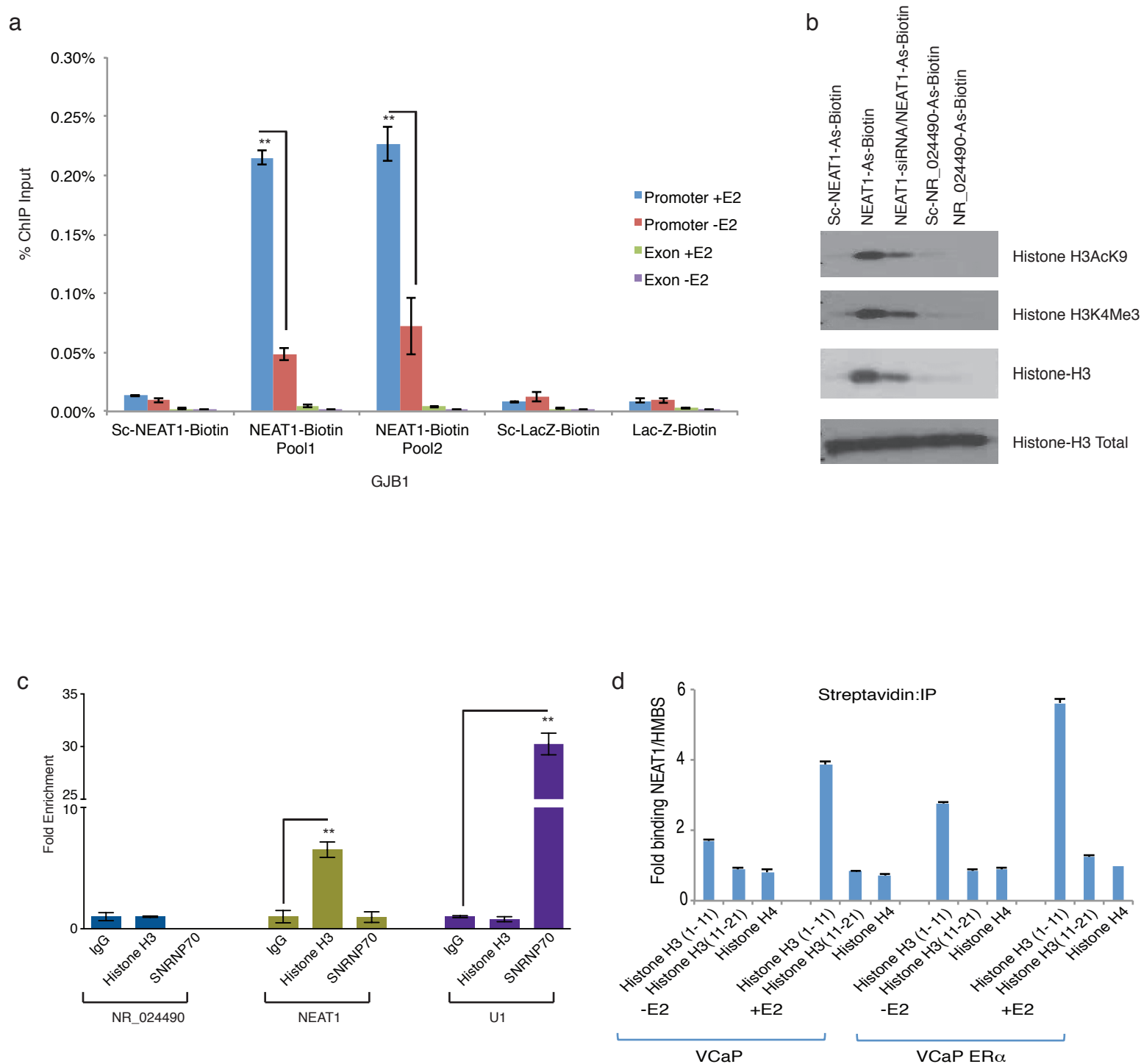
Supplementary Fig. 2

(a) Analysis of NEAT1 using prostate dataset from cBio portal. (b) Representative image depicting NEAT1 expression in benign and tumor tissue by NEAT1 RNA ISH. (c) qRT-PCR showing NEAT1\_2 levels with/without ER $\alpha$  overexpression in different prostate carcinoma cell lines treated with E2 at different time points. Results are expressed as fold enrichment (+E2/-E2). Mean calculated from two independent experiments is shown. Vertical bars represent range of data (d) qRT-PCR analysis for ER $\alpha$ , ER $\beta$  and NEAT1 in VCaP cells transfected with control siRNA and either ER $\alpha$  or ER $\beta$  siRNA. Results are expressed relative mRNA levels. Mean calculated from two independent experiments is shown. Vertical bars represent range of data (e) Representative image depicting NEAT1 expression by RNA ISH in VCaP cells with and without E2 treatment. (f) Chromatin immunoprecipitation followed by quantitative PCR to study ER $\alpha$  recruitment to NEAT1 promoter in VCaP ER $\alpha$  cells with/without E2 (10nM) treatment. qPCR of ChIP-elute was performed with primers spanning the binding regions identified by ER $\alpha$  ChIP Seq data. Results are expressed as percentage of input calculated from two independent experiments. Vertical bars represent range of data. (g) Recruitment profiles of endogenous ER $\alpha$  to promoter regions of NEAT1 by CHIP followed by quantitative PCR in NCI-H660 cells. Results are expressed as fold recruitment. Mean calculated from two independent experiments is shown. Vertical bars represent range of data.



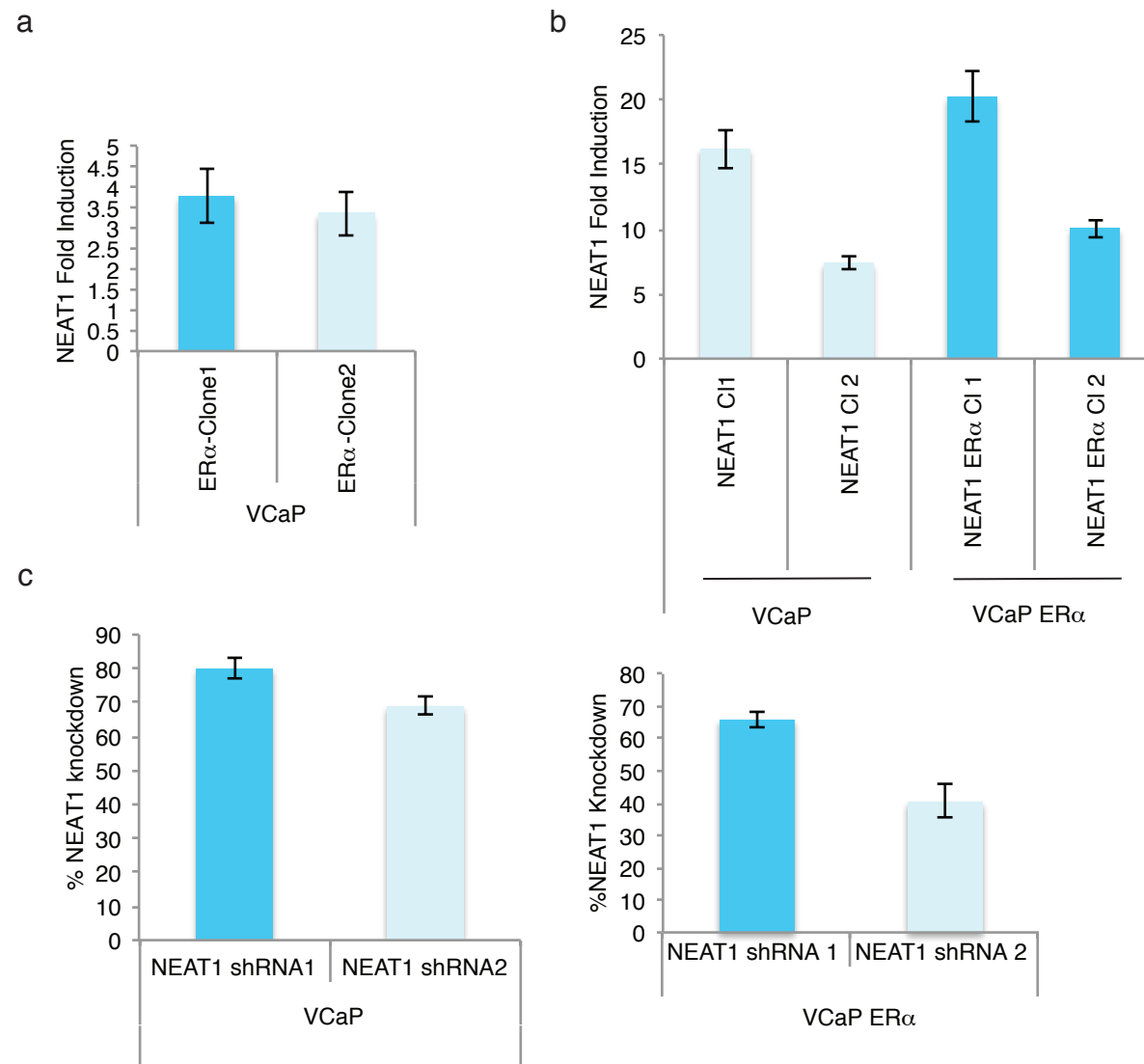
Supplementary Fig. 3

(a) Network representation of NEAT1 signature, derived from genes overexpressed in VCaP NEAT1 cells over vector control cells, across different prostate cancer datasets using OncoPrint concept analysis. (b) Network representation of NEAT1-ER $\alpha$  signature, derived from common target genes overexpressed in VCaP ER $\alpha$  (ER $\alpha$  signature) and NEAT1 correlated genes across prostate cancer datasets from OncoPrint (NEAT1 signature) cells, across different cancer datasets using OncoPrint concept analysis. Each node represents a concept the NEAT1-ER $\alpha$  signature is associated to at a greater than 3-fold odds-ratio. Node size reflects the concept size, i.e. the number of genes in each concept; red and green colors represent correlation with over- or under-expressed genes in the concept respectively; and edge thickness represents the odds-ratio between concepts, ranging from 1.2 to 637. The border color of each node represents the tumor type. (c) inset: Expression of ER $\beta$  in different prostate cancer cell lines in comparison to MCF7. Bottom panel: Expression of PSMA in LnCaP, PC3, VCaP and NCI-H660 cells with ER $\beta$  knock out. Results are expressed as relative mRNA levels from a representative experiment performed in triplicate (n = 3).



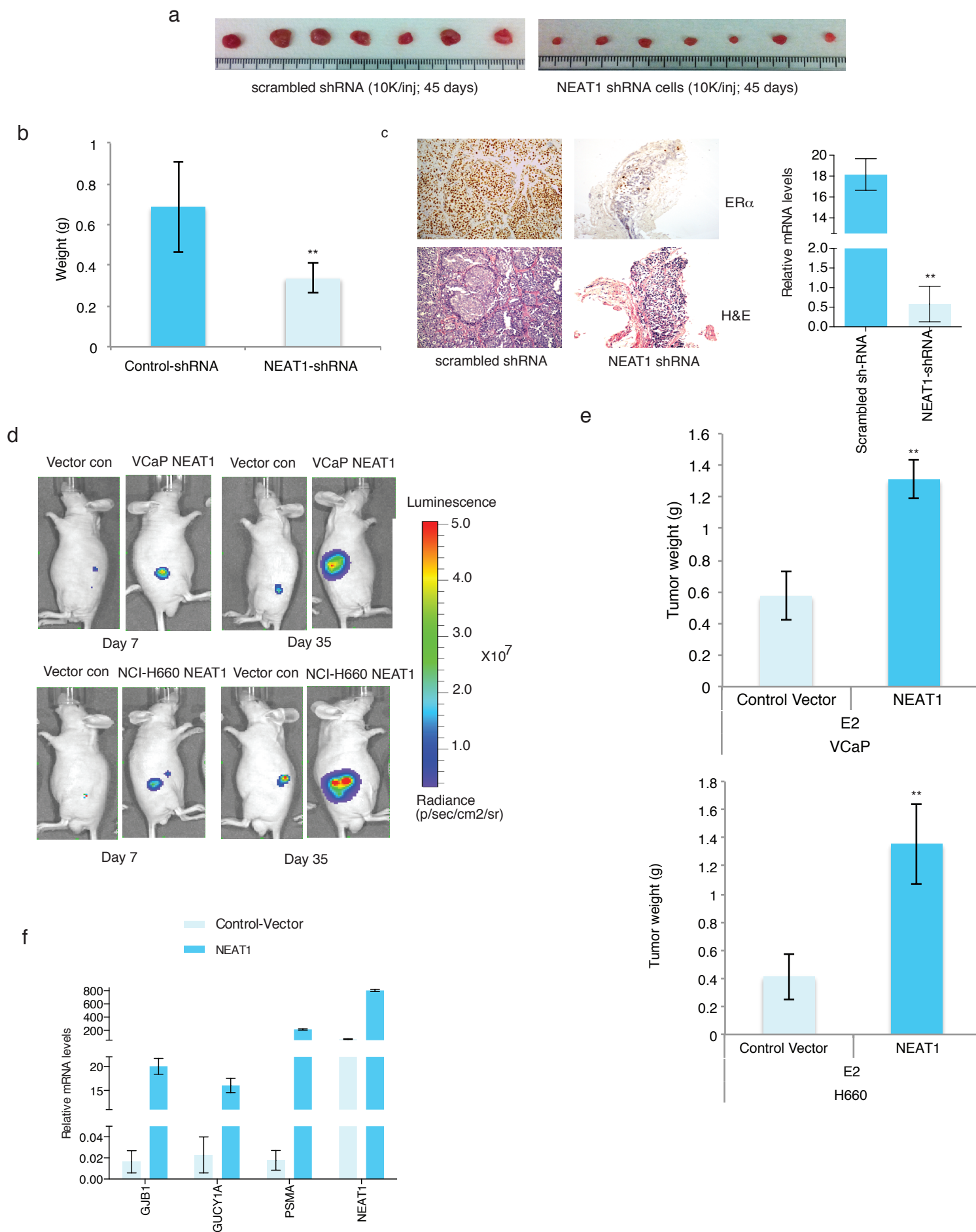
Supplementary Fig. 4

(a) Quantitative analysis of NEAT1 ChIP in VCaP cells with and without E2 treatment. Recruitment profiles of NEAT1 to GJB1 is shown. Results are expressed as the percentage of input calculated from two independent experiments. Error bars represent the range of data. \*\*  $p < 0.01$ , Student's  $t$  test. Results were reproducible between representative experiments. (b) NEAT1 binds to Histone H3 and active histone H3 modifications including, H3Ack9 and H3K4Me3 in NCI-H660 cells. (c) RIP was performed in VCaP ER $\alpha$  cells with anti Histone H3, Normal Rabbit IgG and anti-SNRNP70 as the immunoprecipitating antibody. The figure shows the qPCR data with the purified RNA using primers specific for NR\_024490, NEAT1 and U1 snRNA. Mean calculated from two independent experiments is shown. Vertical bars represent range of data (d) NEAT1 specifically recognizes histone H3. Nuclear lysates from VCaP and VCaP ER $\alpha$  cells treated with either vehicle or E2 were used in a streptavidin-biotin pull down assay using biotinylated histone peptides. RNA bound to streptavidin beads was recovered using Trizol and reverse transcribed to obtain cDNA. Level of immunoprecipitated NEAT1 was determined by quantitative PCR. Mean $\pm$ s.d calculated from three technical replicates is shown. Results were reproducible between representative experiments.



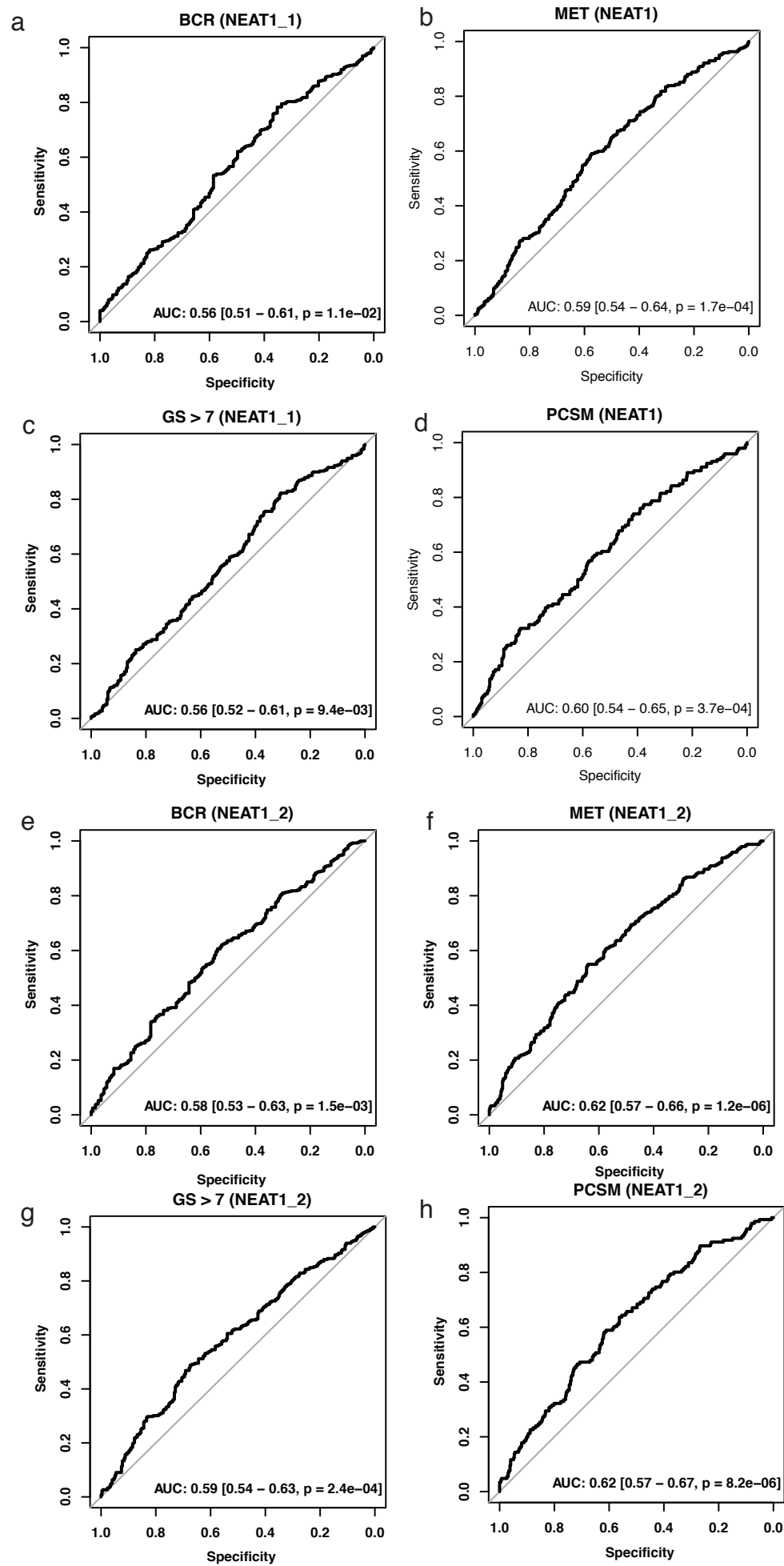
Supplementary Fig. 5

(a) NEAT1 fold induction in VCaP cells overexpressing ER $\alpha$  (b) NEAT1 fold induction in VCaP and VCaP ER $\alpha$  cells overexpressing NEAT1 (c) % knockdown of NEAT1 in VCaP and VCaP ER $\alpha$  cells expressing scrambled shRNA and NEAT1 shRNA. Mean $\pm$ s.d calculated from three independent experiments is shown. Results were reproducible between representative experiments.



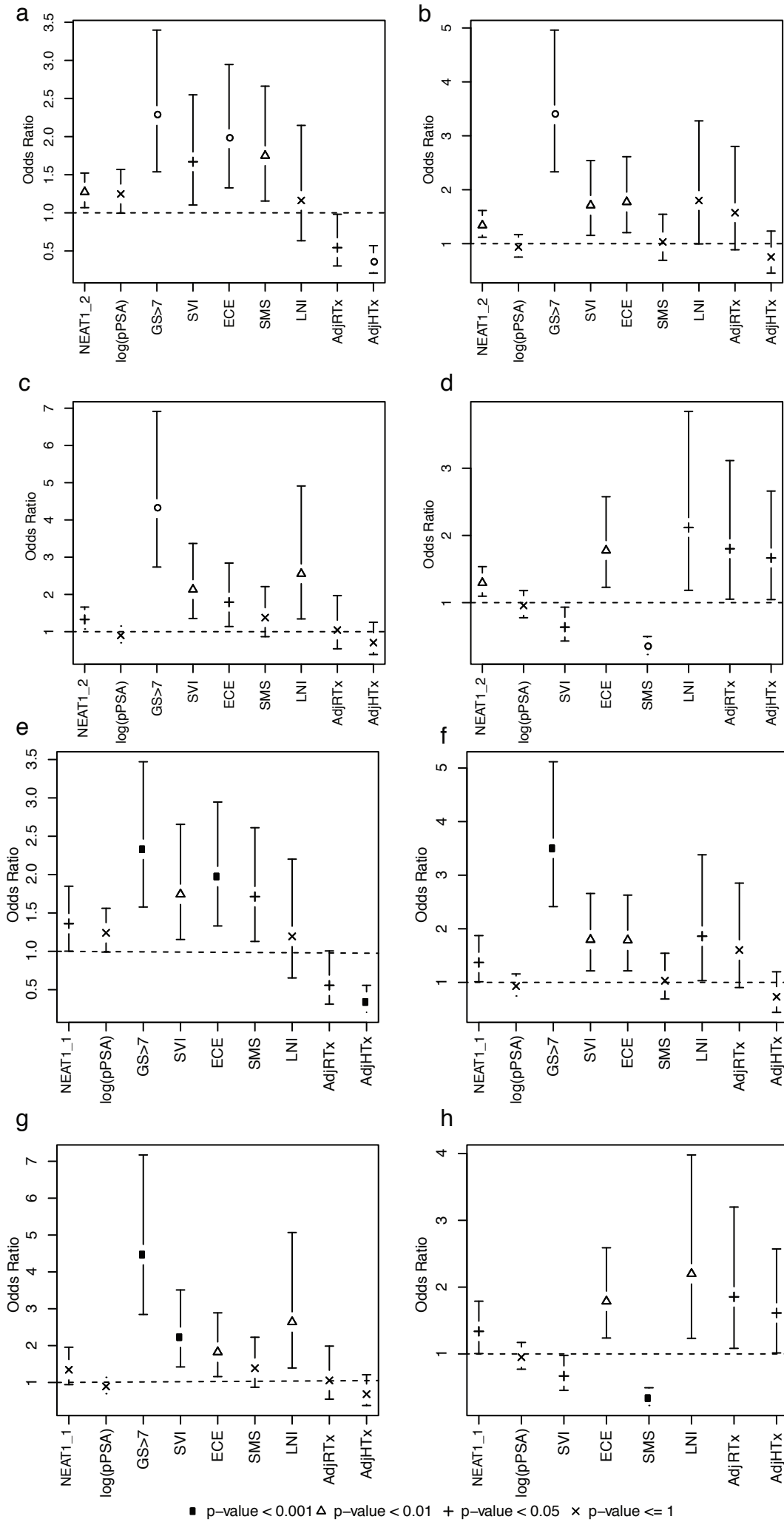
Supplementary Fig. 6

(a) Representative images of tumors derived from mice injected with VCaP ER $\alpha$  cells expressing scrambled shRNA or NEAT1 shRNA. (b) The average tumor weight is shown. Mean $\pm$ s.d is shown, \*\*  $p < 0.01$ , Student's  $t$ -test. (c) Representative immunohistochemistry on the formalin fixed paraffin embedded tissues for ER $\alpha$ . The lower panel shows the H&E staining for the tumors and on the right we see qRT-PCR data for expression of NEAT1 in the xenografts. Data is presented as mean $\pm$ s.d from a representative experiment performed in triplicate ( $n = 3$ ), \*\*  $p < 0.01$ . (d) Bioluminescent imaging on Day 7 and Day 35 in the mice injected with VCaP vector control and VCaP NEAT1 cells (top panel) and NCI-H660 vector con and NEAT1 expressing cells (bottom panel). (e) The average weight of tumors from VCaP vector con and NEAT1 expressing group (top panel) and from NCI-H660 vector con and NEAT1 expressing group (bottom panel). Results are expressed as the means $\pm$ s.d. of three independent experiments. Statistical analysis was performed using Student's  $t$ -test and \*\*  $p \leq 0.01$ . (f) qRT-PCR analysis of relative mRNA levels of 3 ER $\alpha$  NEAT1 signature genes in VCaP vector control and VCaP NEAT1 xenograft tissues; Results are expressed as relative mRNA levels from two independent experiments (cDNA preps). Results were reproducible between representative experiments.



Supplementary Fig. 7

(a-d) AUCs and 95% confidence intervals for the expression of NEAT1\_1 transcript predicting BCR (a), MET (b) GS > 7 patient outcomes (c) and PCSM (d) and NEAT1\_2 transcript predicting BCR (e), MET (f), GS > 7 patient outcomes (g) and PCSM (h). p-values calculated using the Wilcoxon signed-ranked test indicate that both the long and short forms of NEAT1 are found to be significant prognosticators for each outcome.



Supplementary Fig. 8

Multivariable odds ratio forest plots for expression of NEAT1\_1 and NEAT1\_2 transcript.

Forest plots show (a) BCR, (b) MET, (c) PCSM and (d) GS > 7 multivariable odds ratios for NEAT1\_2 and (e) BCR, (f) MET, (g) PCSM and (h) GS > 7 multivariable odds ratios for NEAT1\_1 adjusted for clinicopathologic factors and adjuvant treatment (n = 594). NEAT1 is found to contribute significant independent information for the prognostication of each endpoint.



**Supplementary Table 1: Patient characteristics for the pooled Mayo nested case-control and Mayo case-cohort datasets.**

|           | %  |
|-----------|----|
| BCR       | 68 |
| MET       | 41 |
| PCSM      | 25 |
| GS > 7    | 50 |
| pT3+      | 68 |
| LNI       | 18 |
| SMS       | 62 |
| SVI       | 42 |
| ECE       | 53 |
| pPSA > 20 | 29 |
| AdjHTx    | 33 |
| AdjRTx    | 12 |

**Supplementary Table 1: Patient characteristics for the pooled Mayo nested case-control and Mayo case-cohort datasets.**

Biochemical recurrence (BCR), metastatic recurrence (MET), prostate cancer specific mortality (PCSM), Gleason score (GS) > 7, pathological tumor stage 3 or greater (pT3+), Lymph Node Invasion (LNI), Surgical Margin Status (SMS) positive, Seminal Vesicle Invasion (SVI), Extra Capsular Extension (ECE), preoperative PSA (pPSA), adjuvant hormone therapy, and adjuvant radiation therapy are shown.

**Supplementary Table 2: Clinical information of the patient samples used to derive correlation between NEAT1 and ER $\alpha$  expression**

| Sample ID | Age  | Diagnosis                  | Sample Type             | Site       | Overall Gleason Score | Treatment              |
|-----------|------|----------------------------|-------------------------|------------|-----------------------|------------------------|
| 10680_B   | 72   | Benign                     | Prostatectomy           | Prostate   | NA                    | NA                     |
| 15489_B   | 73   | Benign                     | Prostatectomy           | Prostate   | NA                    | NA                     |
| 16748_B   | 67   | Benign                     | Prostatectomy           | Prostate   | NA                    | NA                     |
| 20870_B   | 62   | Benign                     | Prostatectomy           | Prostate   | NA                    | NA                     |
| 21090_B   | 52   | Benign                     | Prostatectomy           | Prostate   | NA                    | NA                     |
| 21017_B   | 72   | Benign                     | Prostatectomy           | Prostate   | NA                    | NA                     |
| 21070_B   | 79   | Benign                     | Prostatectomy           | Prostate   | NA                    | NA                     |
| 21811_B   | 77   | Benign                     | Prostatectomy           | Prostate   | NA                    | NA                     |
| PM0_B     | 55   | Benign                     | Prostatectomy           | Prostate   | NA                    | NA                     |
| 15489_T   | 73   | Prostate adenocarcinoma    | Prostatectomy           | Prostate   | 7                     | Hormone Naïve          |
| 15508_T   | 70   | Prostate adenocarcinoma    | Prostatectomy           | Prostate   | 9                     | Hormone Naïve          |
| 15969_T   | 64   | Prostate adenocarcinoma    | Prostatectomy           | Prostate   | 7                     | Hormone Naïve          |
| 16288_T   | 67.6 | Prostate adenocarcinoma    | Prostatectomy           | Prostate   | 7                     | Hormone Naïve          |
| 16308_T   | 67   | Prostate adenocarcinoma    | Prostatectomy           | Prostate   | 9                     | Hormone Naïve          |
| 18208_T   | 49   | Prostate adenocarcinoma    | Prostatectomy           | Prostate   | 7                     | Hormone Naïve          |
| 20730_T   | 49   | Prostate adenocarcinoma    | Prostatectomy           | Prostate   | 7                     | Hormone Naïve          |
| PM0       | 55   | Metastatic prostate Cancer | Rapid Autopsy           | Liver      | NA                    | Chemotherapy           |
| PM59      | 77   | Metastatic prostate Cancer | Biopsy                  | Liver      | NA                    | ADT, Chemotherapy      |
| PM90      | 62   | Metastatic prostate Cancer | Biopsy                  | Liver      | NA                    | ADT, Chemotherapy      |
| PM159     | 63   | Metastatic prostate Cancer | Rapid Autopsy           | Lymph node | NA                    | ADT, Chemotherapy      |
| PM89      | 89   | Metastatic prostate Cancer | Biopsy                  | Lymph node | NA                    | ADT, Chemotherapy      |
| PM169     | 66   | Metastatic prostate Cancer | Biopsy                  | Bone       | NA                    | ADT                    |
| PM195     | 85   | Metastatic prostate Cancer | Transurethral Resection | Prostate   | NA                    | ADT, XRT, Chemotherapy |

ADT-Androgen Deprivation Therapy  
XRT-Radiation Therapy

**Supplementary Table 3: Sequence of siRNAs used in this study**

| <b>Target</b>           | <b>Seq.</b>  |
|-------------------------|--|
| siNEAT1                 | UGGUAAUGGUGGAGGAAGAUU  |
| siNEAT1                 | GUGAGAAGUUGCUUAGAAAUU  |
| siNEAT1                 | GGAGGAGUCAGGAGGAAUAAU  |
| siNEAT1_2               | CCAAAUAGGCUUACAGAUAAU  |
| siNEAT1_2               | AGAGAGAAGUUGUGGAGAAUU  |
| ESR1 ON-TARGETplus      | GAUCAACGCUCUAAGAAG<br>GAAUGUGCCUGGCUAGAGA<br>GAUGAAAGGUGGGAUACGA<br>GCCAGCAGGUGCCCUACUA                                |
| ESR1 Accell             | UAUUCAUGUUAAGAUACUA<br>GGAAGGUUUUACAUAUUUC<br>GCCUGGUGAUUAUUCAUUU<br>CCGUAAUGAUUCUAUAAUG                               |
| ESR2 ON-TARGETplus      | GGAAUUGCGUAGAAGGAU<br>UUCAAGGUUUCGAGAGUUA<br>GCACGGCUCCAUAUACUA<br>GAACCCACAGUCUCAGUGA                                 |
| AR ON-TARGETplus        | GAGCGUGGACUUUCCGGAA<br>UCAAGGAACUCGAUCGUAU<br>CGAGAGAGCUGCAUCAGUU<br>CAGAAAUGAUUGCACUAUU                               |
| piLenti-NEAT1 siRNA-GFP | TCATGGACCGTGGTTTGTACTATAGTGT<br>GTTCTTAGCCTGATGAAATAACTTGGGGC<br>GTGAGAAGTTGCTTAGAACTTTCC<br>CTGGTATGTTGCTCTGTATGGTAAG |
| iLenti-si-scrambled     | CAACCCGCTCCAAGGAATCG   |

**Supplementary Table 4: Primer sequences used in this study**

| <b>Gene</b>         | <b>Sequence (5' --&gt; 3')</b>  |
|---------------------|---|
| ERbeta              | ERbeta F: 5' – CTGCTGAGTCTTGGCTGTCA – 3'<br>ERbeta R: 5' – GGATGTGGCAAAGCACTACA – 3'                                  |
| AR                  | AR F: 5' – CCAGGGACCATGTTTTGCC – 3'<br>AR R: 5' – CGAAGACGACAAGATGGACAA – 3'<br>AR F: 5' – CGAAGACGACAAGATGGACAA – 3' |
| AR                  | AR R: 5' – CCAGGGACCATGTTTTGCC – 3'   |
| STAT3               | STAT3 F: 5' – ACCAGCAGTATAGCCGCTC – 3'<br>STAT3 R: 5' – GCCACAATCCGGGCAATCT – 3'                                      |
| TMPRSS2             | TMPRSS2 F: 5' – GGACAGTGTGCACCTCAAAGAC – 3'<br>TMPRSS2 R: 5' – TCCCACGAGGAAGGTCCC – 3'                                |
| ESR1 (ER $\alpha$ ) | ESR1_Lisa F: 5' – GCTGTTCTTCTTAGAGCGTTTGA – 3'<br>ESR1_Lisa R: 5' – GAAAGGTGGGATACGAAAAGACC – 3'                      |
| NEAT 1              | NEAT1_2 F: 5' – TTTGTGCTTGGAAACCTTGCT – 3'<br>NEAT1_2 R: 5' – TCAACGCCCAAGTTATTTTC – 3'                               |
| NEAT 1_2            | NEAT1v2 F: 5' – TCTCCATTTCCCATCTGAG – 3'<br>NEAT1v2 R: 5' – CAGCCACAGAAAAGGGAGAG – 3'                                 |
| HMBS                | HMBS F: 5' – AGCTTGCTCGCATAACAGACG – 3'<br>HMBS R: 5' – AGCTCCTTGGTAAACAGGCTT – 3'                                    |
| HPRT                | HPRT F: 5' – GAAGTTTTGTTCTGTCCTGGAA – 3'<br>HPRT R: 5' – GGGAACTGCTGACAAAGATTC – 3'                                   |
| EHF                 | EHF F: 5' – GGACCAAGTACCAGGTGTGG – 3'<br>EHF R: 5' – GCTGCAAGTTGCTGTAGAGG – 3'  |
| PPM1E               | PPM1E F: 5' – CCCGAACCTGAACTGGTAGA – 3'<br>PPM1E R: 5' – CTCCTCCTCCTCACCCCTCA – 3'                                    |
| SIM2                | SIM2 F: 5' – GGCTACTTGAAGATCAGGCAGT – 3'<br>SIM2 R: 5' – TCCAGGAATATCAGCTTCAGG – 3'                                   |
| ADRB1               | ADRB1 F: 5' – CGAGACCCTGTGTGTCATTG – 3'<br>ADRB1 R: 5' – ACTTGGGGTTCGTTGTAGCAG – 3'                                   |
| HPN                 | HPN F: 5' – GTCCCGATGGCGAGTGTT – 3'<br>HPN R: 5' – AGGGCAATATCGTTGCTGTT – 3'  |
| PLA2G7              | PLA2G7 F: 5' – TCATCAGCATGGGTCAACAAAA – 3'<br>PLA2G7 R: 5' – CCAAAGGGTGTCAAGGCGAT – 3'                                |
| PDLIM3              | PDLIM3 F: 5' – CCAACCTGTGTCCTGGAGAT – 3'<br>PDLIM3 R: 5' – TTGAGACACAGCTGGTGAGC – 3'                                  |
| AMACR               | AMACR F: 5' – TCCGGTTCTGACTTTTGAGG – 3'<br>AMACR R: 5' – CGGCTGAATCCAAATCTTC – 3'                                     |
| RTN1                | RTN1 F: 5' – GACCTGTTGTATTGGCGGGAC – 3'<br>RTN1 R: 5' – GTAGATGCGGAACTGATGGTG – 3'                                    |
| GJB1                | GJB1 F: 5' – GAAAATGCTACGGCTTGAGG – 3'<br>GJB1 R: 5' – TAGACGTGCACTTGACCAG – 3'                                       |
| SPDEF               | SPDEF F: 5' – CAGTGCCCGGTCATTGACA – 3'<br>SPDEF R: 5' – CAGCCGGTATTGGTGCTCT – 3'                                      |
| ARHGAP6             | ARHGAP6 F: 5' – TTTGGAATGCCCTTATCCCAAG – 3'<br>ARHGAP6 R: 5' – TCTGCTCGTCCCTCTGCAA – 3'                               |
| CHGB                | CHGB F: 5' – GAGCCTCTATCCCTCCGACAG – 3'<br>CHGB R: 5' – CCCTCGCTCCCCTTTTTGA – 3'                                      |
| PRAC                | PRAC F: 5' – CTAGCCTAAGGCGTGCAAAC – 3'<br>PRAC R: 5' – CCGGTCCTTGATCTGAGAAA – 3'                                      |
| ACPP                | ACPP F: 5' – GCTTCCCCTCTACAGGCTTT – 3'<br>ACPP R: 5' – GCAGAAACAAGAAGCCAAGG – 3'                                      |
| PSMA/FOLH1          | PSMA F: 5' – CATAGTGCTCCCTTTTGATTGTC – 3'<br>PSMA R: 5' – CTCTCACTGAACTTGGAAAGCAAT – 3'                               |
| B3GAT1              | B3GAT1 F: 5' – CCTGGCGTGGTCTACTTCG – 3'<br>B3GAT1 R: 5' – GCAGGTTGACGGCAAATCC – 3'                                    |

ALDH1A1 F: 5' – GAAGAAAGAAGGGGCCAAAC – 3'  
ALDH1A1 R: 5' – CAATGCGCATCTCATCTGTAA – 3'  
TRPM8 F: 5' – GAAACCTGTGCGACAAGCACA – 3'  
TRPM8 R: 5' – GAGGACAAAGACCAGCGAGT – 3'  
GUCY1A3 F: 5' – GATTGCAGCGAGTTTGTGAA – 3'  
GUCY1A3 R: 5' – ATCAGCCTTCTGATGCCATT – 3'  
ERG F: 5' – TTGTGAGTGAGGACCAGTCG – 3'  
ERG R: 5' – CCTGGCTAGGGTTACATTCC – 3'  
NPY F: 5' – GCTAGGTAAACAAGCGACTGG – 3'  
NPY R: 5' – CTGCCTGGTGATGAGGTTG – 3'  
KLK2 F: 5' – CACAACCTGTTTGAGCCTGA – 3'  
KLK2 R: 5' – CCCAGGACCTTCACAACATC – 3'  
LDHB F: 5' – TGGTATGGCGTGTGCTATCAG – 3'  
LDHB R: 5' – TTGGCGGTCACAGAATAATCTTT – 3'  
CRISP3 F: 5' – AAAACCCTGGATTGAAAGTGAA – 3'  
CRISP3 R: 5' – AGCCAGATGATTGGGAAGAA – 3'  
ACPP F: 5' – GCTTCCCCTCTACAGGCTTT – 3'  
ACPP R: 5' – GCAGAAACAAGAAGCCAAGG – 3'  
STEAP2 F: 5' – CAAGCGCGACAACAGGTTATT – 3'  
STEAP2 R: 5' – CAGAGAGTAAAGAGTCGTAGGGG – 3'  
PRAC F: 5' – AAGGACCGGCCCATCTTACTA – 3'  
PRAC R: 5' – CCTGGTCTCGCCCAGTAGA – 3'  
CLDN8 F: 5' – CAACCCATGCCTTAGAAATCGC – 3'  
CLDN8 R: 5' – TCACGCAATTCATCCACAGTC – 3'  
STEAP1 F: 5' – CCCTTCTACTGGGCACAATACA – 3'  
STEAP1 R: 5' – GCATGGCAGGAATAGTATGCTTT – 3'  
KLK4 F: 5' – TCAGCCGCACACTGTTTCC – 3'  
KLK4 R: 5' – GGGTCTGTTGTA CTCTGGGTG – 3'  
TMPRSS2 F: 5' – GGACAGTGTGCACCTCAAAGAC – 3'  
TMPRSS2 R: 5' – TCCCACGAGGAAGGTCCC – 3'

NR\_024490 F: 5' – TTCCTGTGCTAACCTTCGTG – 3'  
NR\_024490 R: 5' – GGTACCTTCACAGCGTCTCC – 3'  
FR349599 F: 5' – CCTGGCTTCACCGCATTCC – 3'  
FR349599 R: 5' – AGGGTGGTCCTGAGAGTGGT – 3'  
FR330851 F: 5' – TCATTGCATGGTTGGAAATG – 3'  
FR330851 R: 5' – CAACTTTCTGCCTTCAACTGC – 3'  
NR\_026919 F: 5' – TGGGCTCTGACCTCTGTACC – 3'  
NR\_026919 R: 5' – CTGATAAATGTCCCCGTGCT – 3'  
NR\_027334 F: 5' – CAGCCCTACCTGTCCTGATG – 3'  
NR\_027334 R: 5' – ACTGAGCCTCCA ACTCCAGA – 3'  
U1 snRNA F: 5'-GGG AGA TAC CAT GAT CAC GAA GGT-3'  
R: 5'-CCA CAA ATT ATG CAG TCG AGT TTC CC-3'

Primers used in ChIP Assay

ESR1\_P\_1 F: 5' – GTGAAACCCCGTCTCTACCA – 3'  
ESR1\_P\_1 R: 5' – TGGGAAGACAACCTGTAGGG – 3'  
ESR1\_P\_2 F: 5' – AGCAGGCCAATCTAGAAGCA – 3'  
ESR1\_P\_2 R: 5' – CAGCAATGGAAGGACAGA ACT – 3'  
ESR1\_P\_3 F: 5' – AATGGAATGGACTCGAATGG – 3'  
ESR1\_P\_3 R: 5' – ATTGCAATCCATTTCTTTTCG – 3'  
ESR1\_P\_4 F: 5' – TGGAATCGAATCACATGGAA – 3'  
ESR1\_P\_4 R: 5' – CCATTCCACACCTCTCCAGT – 3'

ESR1\_P\_5 F: 5' – GGCATCGAATGAAATGGAAT – 3'  
 ESR1\_P\_5 R: 5' – TTCAAATAAATTCCGCTCGTG – 3'  
 ESR1\_P\_6 F: 5' – CCTCGAGCGGAATTTATTTG – 3'  
 ESR1\_P\_6 R: 5' – TCGATTTTCGTTCCCTTTGAT – 3'  
 ESR1\_P\_7 F: 5' – TGGAGTGTAACGGGATGATG – 3'  
 ESR1\_P\_7 R: 5' – TCTCCATTCGAGTCCATTCC – 3'  
 ESR1\_P\_8 F: 5' – GAATGGAATGGAAGGCAATG – 3'  
 ESR1\_P\_8 R: 5' – CAAGCCACTTCAATCCCCTA – 3'  
 ESR1\_P\_9 F: 5' – AATAGAATGGAACGGCATCG – 3'  
 ESR1\_P\_9 R: 5' – CCATTCGAATCCAATACTCA – 3'  
 ESR1\_P\_10 F: 5' – TGAAATGGAGCGCATTAGAA – 3'  
 ESR1\_P\_10 R: 5' – TGTCCATTCCATTTGATTGC – 3'  
 ESR1\_P\_11 F: 5' – GCTCCAGCATTCTGACCTCT – 3'  
 ESR1\_P\_11 R: 5' – CAGGAGCAACTCTGGGTCTC – 3'

PSMA-P\_1 F: 5' – TGCACGGCCTCTCTCACGGA – 3'  
 PSMA-P\_1 R: 5' – GGCTATGTCTGGCTACTGTCTTA – 3'  
 PSMA-P\_2 F: 5' – TCGAGAAATCGAGACCATCC – 3'  
 PSMA-P\_2 R: 5' – ACTCTGTCACCAGGCTCCAG – 3'  
 PSMA-F:5'-GGGTCTTGATGCTGTGGTCT-3'  
 PSMA-R:5'-ATCTTTCCCCTATGCCTGGT-3'

B3GAT1-P\_1 F: 5' – ACCCGAGCTGCTAATGGTC – 3'  
 B3GAT1-P\_1 R: 5' – GGTGGGGAGGTGATACCAAT – 3'  
 B3GAT1-P\_2 F: 5' – CCCCAGATCTCGGCTCTC – 3'  
 B3GAT1-P\_2 R: 5' – CTTTGAGAGAGGGCTGCCAAG – 3'  
 B3GAT1-P\_3 F: 5' – CACTGGTAGGGTGCCTCTGT – 3'  
 B3GAT1-P\_3 R: 5' – CCCGAATACAGGTGTCCAAG – 3'  
 B3GAT1-P\_4 F: 5' – TCTAGGGTCTCCCTCCTTCC – 3'  
 B3GAT1-P\_4 R: 5' – GCAGGAAAGCTGATGGAAAA – 3'

GJB1-P\_1 F: 5' – TCCAGCTCAGTTTTGCCTTT – 3'  
 GJB1-P\_1 R: 5' – GGGAGGAGGAACAGTGTGAG – 3'  
 GJB1-P\_2 F: 5' – CGGCCCTGTCATACAGTTTT – 3'  
 GJB1-P\_2 R: 5' – ATTGTCACCCACCCATGTTT – 3'  
 GJB1-F: 5'-GAAAATGCTACGGCTTGAGG-3'  
 GJB1-F: 5'-TAGACGTGCGCACTTGACCAG-3'

NEAT1\_P\_2 F: 5' – GGCAGTGACCCTGACAAGTT – 3'  
 NEAT1\_P\_2 R: 5' – TCTGAAGGAGCCTTTTCTGC – 3'  
 NEAT1\_P\_3 F: 5' – CCATCTGACCTTGGCACTTT – 3'  
 NEAT1\_P\_3 R: 5' – CAACCCACCTTGGTCTGACT – 3'  
 NEAT1\_P\_4 F: 5' – GGGAACCTCCCTTCCTCAGTC – 3'  
 NEAT1\_P\_4 R: 5' – CAGCCTCCTGACCACAACCTC – 3'  
 NEAT1\_P\_1 F: 5' – AATTTTCCAGATGTCCTGCC – 3'  
 NEAT1\_P\_1 R: 5' – AACAGTGCTTTTTGGGATCG – 3'

ER\_P\_NT-NEAT1\_1 F: 5' – TCATTGGTCATGGCTTAGCA – 3'  
 ER\_P\_NT-NEAT1\_1 R: 5' – AGCCATTTTGTCTCCTGCAC – 3'  
 ER\_P\_NT-NEAT1\_2 F: 5' – ACTATTTCAACCGCCACGAG – 3'  
 ER\_P\_NT-NEAT1\_2 R: 5' – TGCCTGAGGGCTCTAGTCAT – 3'

FOR: GGG AGA TAC CAT GAT CAC GAA GGT  
 REV: CCA CAA ATT ATG CAG TCG AGT TTC CC

U1 snRNA

## Supplementary Table 5: Biotin TEG antisense probes

### Biotin TEG probes:

| Sequence Name | Sequence (5'-3')     |
|---------------|----------------------|
| NEAT1_scr1    | gagaacatcgaattagcgtc |
| NEAT1_scr2    | gactatcagacgcctaagat |
| NEAT1_scr3    | ggtacgtaacgaggaagcga |
| NR_024490_1   | ttaaattcttggcgctgtct |
| NR_024490_2   | aagtcttcataataaccctt |
| NR_024490_3   | actcagtccaagtcattact |
| LacZ_1        | tcacgacgttgtaaacgac  |
| LacZ_2        | gctgatttgtgtagtcggtt |
| LacZ_3        | ttaccttgtggagcgacat  |
| HOTAIR_1      | atthtaggaggcccaaacag |
| HOTAIR_2      | tgttcactctggcaagagat |
| HOTAIR_3      | actttgccagattaaacgt  |
| NEAT1_185     | tgccgatatttccatgcag  |
| NEAT1_488     | agcccttggctcgaaaaaa  |
| NEAT1_800     | aagcgttggccaatgttgtc |
| NEAT1_1161    | tcgcatgaggaacactata  |
| NEAT1_1516    | tcagcatctgaaaacctt   |
| NEAT1_1829    | cacaacacaatgacaccctt |
| NEAT1_2195    | actgtatcttaaccaacc   |
| NEAT1_2555    | ccaggaggaagctggtaaag |
| NEAT1_2939    | gatgtgttctaaggcacga  |
| NEAT1_3325    | ccattggattactttacca  |
| NEAT1_3691    | ttatttgctgtaaagggg   |

## **Supplementary Methods**

### **Tissues:**

The prostate cancer tissue microarrays include 64 benign, 16 high grade PIN, 292 adenocarcinoma and 42 neuroendocrine prostate cancer specimens. Tissues were obtained from radical prostatectomy series at the Weill Cornell Medical College. All samples were collected with informed consent of the patients and under an Institutional Review Board approved protocol. Hematoxylin and eosin (H&E) stained FFPE and frozen sections were reviewed by study pathologist (M.A.R./J.M) to identify regions of high density cancer foci, or high grade prostate intraepithelial neoplasia or lack of tumor.

### **Immunohistochemical staining of Tissue microarrays:**

Sections were deparaffinized with xylene and rehydrated using graded ethanol. The hydrated sections were boiled for 10 minutes in 0.01mol/L citrate buffer and cooled for 30 minutes at room temperature to expose antigenic epitopes. Tissue slides were blocked for 30 min at room temperature with 2% normal goat serum and 1% BSA in PBS for 30 minutes. Tissue cores were incubated with rabbit monoclonal antihuman-ER $\alpha$  antibody (RM-9101, Thermo scientific) at a dilution of 1:100 and incubated overnight at room temperature. The sections were washed thrice with 0.05% Tween in PBS for 10 minutes, incubated with secondary antibody for 1 hour, washed thrice with 0.05% Tween in PBS for 10 minutes, developed with 3,3'-diaminobenzidine-H<sub>2</sub>O<sub>2</sub>, (DAB) and then counterstained with Mayer's hematoxylin. Negative controls were done by replacing the primary antibody with control rabbit IgG or peptide-absorbed ER $\alpha$  antibody. For each run a positive tissue control (breast cancer) was included. Subjective evaluation of ER $\alpha$  protein expression was scored as positive or negative by pathologists



for the study. The same protocol was also followed for immunohistochemical staining on the xenograft tissue sections for ER $\alpha$ .

### **RNA isolation, cDNA synthesis and PCR experiments:**

Total RNA was isolated from frozen prostate tissue samples (for qPCR) and cell lines (for transcriptome sequencing and qPCR) using Trizol (Invitrogen) with DNase I digestion according to manufacturer's instructions. RNA integrity was verified on an Agilent Bioanalyzer 2100 (Agilent Technologies). cDNA was synthesized from total RNA using Superscript III (Invitrogen) and random primers (Invitrogen).

Quantitative RT-PCR was performed using Power SYBR Green Mastermix (Applied Biosystems) on an Applied Biosystems 7900 Fast Real Time PCR machine. All primers were designed using Primer 3 and synthesized by Integrated DNA Technologies. Primer sequences are provided in **Supplementary Table 5**.

### **Statistical analysis for quantitative RT-PCR:**

For quantitative real time PCR, we subtracted the mean CT value from each gene "g" to the mean control value (HMBS) to compute the Delta CT value:

$\Delta CT_g = \overline{CT_g} - \overline{CT_{HMBS}}$ . The standard deviation of this value was calculated as the square

root of the sum of the squares of the standard deviations:  $SD_{\Delta CT} = \sqrt{SD_g^2 + SD_{HMBS}^2}$ . We

then computed  $\Delta \Delta CT_g = 2^{-(\Delta CT_g)}$  for each gene and condition and considered each value

to be within this range  $[2^{-(\Delta CT_g - |SD_{\Delta CT}|)}, 2^{-(\Delta CT_g + |SD_{\Delta CT}|)}]$ . Finally we computed the fold

changed between condition C1 and C2, e.g. C1=with E2 and C2=without E2 as:

$FC = \frac{\Delta \Delta CT_g^{C1}}{\Delta \Delta CT_g^{C2}}$ . The standard deviation of this value was computed according to the rules

of propagation of error, i.e.  $\frac{SD_{FC}}{FC} = \sqrt{\left(\frac{SD_{C1}}{\Delta\Delta CT_g^{C1}}\right)^2 + \left(\frac{SD_{C2}}{\Delta\Delta CT_g^{C2}}\right)^2}$ ; where  $SD_{Ci}$  is the range of  $\Delta\Delta CT_g^i$  for condition  $i$ .

### **Western Blot:**

Cells were fractionated and lysed as described previously. Standard protocols were followed for western blotting<sup>1</sup>. PVDF membranes (GE Healthcare) were used for western blotting and immunoblotted using specific antibodies.

Antibodies and the dilutions used: Anti AR (06-680, Millipore, 1:1000), Anti ER $\alpha$  (AC-066-100, diagenode, 1:1000), Anti Ace-H3 (06-599, Millipore, 1:1000), Anti H3K4me3 (ab8580, Abcam, 1:1000), Anti GAPDH (AB2302, Millipore, 1:10000), Anti Actin (MAB1501, Millipore, 1:1000), Anti Lamin B1 (ab28129, Abcam, 1:1000), Anti Histone H3 (06-755, Millipore, 1:1000), Anti Paxillin (05-417, Millipore, 1:1000), Anti ER $\beta$  (ab288, Abcam, 1:1000).

### **RNA immunoprecipitation (RIP assay):**

RIP assays were performed using Milipore EZ-Magna RIP kit (17-701) according to the manufacturer's instruction. Briefly, cells were lysed in RIP lysis buffer, followed by immunoprecipitation with antibody to Histone H3 (ab1791, Abcam, 5 $\mu$ g), Anti-SNRNP70 (CS203216, Millipore, 5 $\mu$ g) and negative control Normal Rabbit IgG (PP64B, Millipore) with protein A/G magnetic beads. The magnetic bead bound complexes were washed to get rid of unbound materials and the RNA was extracted and subsequently analyzed by qRT-PCR.

**Peptide pull-down assay:**

Nuclear lysates from VCaP and VCaP ER $\alpha$  cells treated with either vehicle or E2 were used in a streptavidin-biotin pull down assay using biotinylated histone peptides<sup>2</sup>. RNA bound to streptavidin beads was recovered using Trizol and reverse transcribed to obtain cDNA. Levels of immunoprecipitated NEAT1 were determined by quantitative PCR.

**RNA sequencing:**

Standard poly-A selected RNA sequencing was done for VCaP, VCaP ER $\alpha$  expressing cells as well as for VCaP cells overexpressing empty vector and VCaP NEAT1 overexpressing cell lines using Illumina TruSeq RNA-seq protocol.

Reads were aligned to the reference genome NCBI36/hg18 without the minor haplotypes and the minor sequences using STAR aligner<sup>3</sup>. Reads mapped to the mitochondrial genome were removed. The expression of each gene (UCSC knownGenes) was computed using mrqQuantifier, part of RSEQtools<sup>4</sup>. The resulting expression data was used to identify variation in gene expression between VCaP and VCaP ER $\alpha$  cells and also between the vector control and NEAT1 expressing cells. We computed the ratio between VCaP and VCaP ER $\alpha$  and control cells and VCaP NEAT1, after adding 1, and selected those genes with a log<sub>2</sub>-fold change greater than 2. Results are reported in **Supplementary dataset 3** and **Supplementary dataset 4**.

**ChIP sequencing:**

ER $\alpha$  ChIP followed by sequencing was performed in VCaP, VCaP + E2, VCaP ER $\alpha$  + E2 expressing cells and in NCI-H660 cells with and without E2 treatment. Cells were

treated with E2 for 48hrs. ChIP experiments were carried out using Millipore EZ-Magna ChIP kit (Catalogue # 17-10086). Briefly  $5-10 \times 10^6$  cells were crosslinked with 1% formaldehyde for 10 min at room temperature. The crosslinking was then quenched with 0.125 M glycine. Chromatin was sonicated in the lysis buffer to 300-500 bp and the extraction of ChIP DNA was done as per the kit protocol.

For ChIP sequencing the concentrations of the ChIP DNA were quantified by Qubit Fluorometer (Invitrogen). ChIP DNA was prepared into libraries and direct sequencing of the ChIP libraries was performed using illumine Genome Analyzer according to standard manufacturers procedures.

#### **ChIP seq data analysis:**

Peak detection for all ChIP-seq experiments was performed with ChIPseeqer<sup>5</sup>, using the same parameters for all datasets (i.e., p-value threshold for peaks= $10^{-5}$ , minimum distance between peaks=100bp). Genomic annotation of ChIP-seq peaks, comparison between ChIP-seq datasets and motifs analysis were performed using the corresponding tools in the ChIPseeqer software.

We ranked the binding sites according to their p-value as determined by ChIPSeeqer and considered the expression levels of the potential target genes. In this case, we defined a target gene if it is within 20KB of the peak and considered only genes whose expression is higher than 1 in at least one condition (either VCAP con or VCAP ER $\alpha$ ).

#### **Association of NEAT1 co-related signature with Oncomine concepts**

Similar to the ER $\alpha$  and NEAT1 signature we also created a NEAT1 gene signature considering the genes that were positively correlated (correlation > 0.5) to NEAT1

expression across prostate cancer datasets in OncoPrint and looking for overlapping genes with the ER $\alpha$  588 gene signature we identified 155 overlapping genes. We defined this NEAT1-ER $\alpha$  signature as an OncoPrint custom concept and determined significantly associated tumor vs normal concepts with odds ratio > 3.0 and  $P < 1 \times 10^{-6}$ . These results are represented as a network using Cytoscape version 2.8.2.

### **Dataset of long non-coding RNAs (lncRNAs):**

We generated a reference set of known ncRNAs from various sources, listed hereafter:

- RefSeq<sup>6</sup>: 6,499 ncRNAs downloaded from UCSC Table Browser by selecting those without protein coding information, i.e. cdsStart=unk and cdsEnd=unk. The dataset was downloaded on 2012.01.31. By selecting those longer than 200nt, we considered 4,637 elements.

- GENCODE v7<sup>7</sup>: We then selected for lincRNA (1,390), snoRNA (1,521), and snRNA (1,943) for a total of 4,854 elements, out of which 1,460 are longer than 200nt. hg19 coordinates converted into hg18 coordinates by liftOver. We removed lncRNAs that were already in the RefSeq data set, by excluding those with at least 25% overlap with a RefSeq lncRNA. This resulted in 859 lncRNAs that are unique to GENCODE.

- lncRNADB.com<sup>8</sup>: We obtained the coordinates of 73 lncRNAs included in the database (personal communication, Marcel Dinger). We then selected those that were not already identified in the previous steps (less than 25% overlap) and longer than 200nt. This resulted in 30 lncRNAs.

- ncRNA.org: We selected different databases provided via the interface table browser: RNAz F\_RNAz\_set1\_90 (36,155)<sup>9</sup>, Jones Eddy (7,218) [ncRNA annotation track for the human genome, version hg16 (July 2003) T.A. Jones, S.R. Eddy ({tajones,eddy}@genetics.wustl.edu)2 March 2004]), RNAPomics (1,051)<sup>10</sup>,

sasaki\_et\_al\_150 (153 )<sup>11</sup>, The names refer to the specific table we used. The total number of elements in this set is: 44,577 of which 6,993 are longer than 200nt. We removed those that were already identified (376), thus the final elements remaining was 6,617.

Cumulatively, the total known ncRNAs from the various databases was 12,143. We classified an lncRNA as intergenic if it did not overlap with any of the transcripts in Ensembl (62,074). According to this definition, about 54% of the lncRNAs (6,850) are intergenic; while the remaining are intronic. To compute the overlap between datasets we used BEDtools<sup>12</sup>.

### **Characterization of the lncRNAs:**

We characterized the lncRNAs according to their potential of being regulated by ER $\alpha$ . Moreover, we considered several histone marks to provide evidence of transcription.

### **Estrogen receptor alpha (ER $\alpha$ ) binding:**

ChIP-sequencing data on two prostate cell line (VCaP ER $\alpha$  and NCI-H660) were used in order to identify the binding sites of the estrogen receptor. The data was analyzed by ChIPseeker and we identified 3,819 ER $\alpha$  binding sites (ERBS) which were then used to classify the lncRNAs. Specifically, we classified an lncRNA as regulated by ER $\alpha$  if an ERBS lies within 5KB upstream to its transcription start site (TSS). According to this definition, 302 (2.49%) intergenic lncRNAs were regulated by 97 (2.54%) ERBS.

We also looked for Estrogen-Responsive Elements (ERE) motifs within the ER $\alpha$  binding sites of ER $\alpha$  regulated lncRNAs. Specifically, we considered both full ERE (137,531) and half ERE (1,966,283) motifs. The location of ERE motifs were obtained from Carrol et

al<sup>13</sup>. Ninety-two out of 97 (95%) ER $\alpha$  regulated intergenic lncRNA had an ERE motif within the binding sites.

We also considered other transcription binding factors that may act as cofactors in estrogen regulation. Specifically we looked at the Activator Protein 1 (AP-1), which is a regulator of gene expression in response to a variety of stimuli. It is a heterodimer composed by several proteins, among which are c-Jun, c-Fos, and JunD. We thus considered the binding sites of these proteins (from the GM12878 Yale TFBS track in UCSC Genome Browser) and identified which are fully contained in ER $\alpha$  binding sites.

### **Histone Marks**

Similarly to the ER $\alpha$  analysis, we characterized the lncRNAs with respect to active marks (H3K4me3 and H3K36me3), and repressive marks (H3K9me3 and H3K27me3), provided by Chinnaiyan et al.<sup>14</sup>. A window of 10Kb was considered to associate a histone mark to an lncRNA.

### **RNA extraction, sample preparation and sequencing:**

For RNA sequencing analysis frozen tissue was cored (1.5 mm biopsy cores) and RNA extracted using TRIzol Reagent (Invitrogen, CA). Tissues were obtained from radical prostatectomy series at the Weill Cornell Medical College. All samples were collected with informed consent of the patients and under an Institutional Review Board approved protocol. The extracted RNA was subjected to DNase treatment using a DNA-free TM Kit (Applied Biosystems/ Ambion, Austin, TX, USA). RNA quality was measured using the RNA 6000 Nano Kit on a Bioanalyzer 2100 (Agilent Technologies, Santa Clara, CA, USA). RNA with RIN (RNA integrity number)  $\geq 8$  was used for subsequent library preparation. Illumina's sample preparation protocol for paired-end sequencing of mRNA

was used, as previously described<sup>15</sup>. The paired end reads were then aligned to the human genome (hg18) using ELAND/CASAVA, as described previously<sup>15,16</sup>.

#### **Differential expression analysis:**

We performed pair-wise differential expression analysis on a set of paired-end RNAseq samples (26 benign prostate, 40 prostate adenocarcinoma, and 7 neuroendocrine prostate adenocarcinoma) in order to prioritize the experimental validation.

**Supplementary dataset 1** shows the details of the sequencing. Briefly, using the Illumina software suite ELAND/CASAVA, reads were simultaneously mapped to the reference genome NCBI36/hg18 without the minor haplotypes and the minor sequences and a splice junction library based on UCSC knownGenes annotation dataset. Reads mapped to the mitochondrial genome were removed. The library was generated using RSEQtools accordingly to the read size<sup>4</sup>. Gene expression (RPKM) was computed on the composite models based on UCSC knownGenes annotation dataset. Raw RPKM values were then log<sub>2</sub>-transformed after adding 1, and the resulting dataset was quantile normalized, using the R software package “limma” (<http://bioinf.wehi.edu.au/limma>).

We performed Wilcoxon test for benign vs. PCa and PCa vs. NEPC on the normalized dataset. The candidates in each list were ranked by p-values, after correction for multiple hypothesis testing<sup>17</sup>. Similarly, we computed the RPKM values for the known lncRNAs and performed the same differential analysis on log<sub>2</sub>-transformed RPKM+1 values.

#### **VCaP and VCaP ER $\alpha$ sequencing:**

Strand Specific sequencing was done for VCaP and VCaP ER $\alpha$  expressing cell lines using deoxy-UTP method for library preparation<sup>18</sup> with some modifications. Briefly, Ribo-Zero rRNA removal kit (RZH1046, Epicentre Biotechnologies, Madison, WI) was used to



remove ribosomal RNA followed by incorporation of deoxy-UTP during second strand cDNA synthesis. Subsequently the uridine-containing strand was destroyed and that enabled identification of the transcript orientation.

Reads from each strand were aligned to the reference genome NCBI36/hg18 without the minor haplotypes and the minor sequences. Reads mapped to the mitochondrial genome were removed. The expression of each gene (UCSC knownGenes) and the lncRNAs identified by our method was computed using RSEQtools<sup>4</sup>. Specifically, we used bgrQuantifier, after generating the bedgraph files from the mapped data. The reference annotation file (UCSC knownGene annotation or the known lncRNA dataset), which includes the coordinates of all the genes from both strands, was first split according to strand information if available. This avoided assigning reads to the wrong gene on the opposite strand when computing the expression levels. The resulting expression data was used to identify variation in gene expression between the control and ER $\alpha$  expressing cells. We computed the ratio between VCaP and VCaP ER $\alpha$ , after adding 1, and selected those genes with a log<sub>2</sub>-fold change greater than 2. Results are reported in **Supplementary dataset 3**.

#### **Preparation of NEAT1 RNA ISH probe:**

The full length NEAT1 gene was cloned in pCRII-TOPO (Invitrogen) vector. The plasmid was digested with NotI (New England Biolabs) and purified with the Qiaquick PCR Purification Kit (Qiagen) according to manufacturer's protocol. In vitro transcription was accomplished using 500ng of linearized plasmid DNA and the MEGAscript SP6 kit (Ambion) as directed by the manufacturer. The resultant RNA was cleaned using the RNeasy kit (Qiagen) using the manufacturer's protocol. 5 $\mu$ g of RNA was mixed with 10 $\mu$ l of buffer A, 5 $\mu$ l of ML DNP reagent (both provided by Ventana-Roche) and water to

50 $\mu$ l. The reaction was incubated at 37°C for two hours. The labeled RNA was cleaned with the RNeasy Kit (Qiagen). 50-250ng/ml of probe was mixed in Ribohybe solution (Ventana-Roche) and 100ul of the probe was used for each slide. RNA in situ hybridization on FFPE slides was performed using an automated protocol developed for the Discovery XT automated staining system (Ventana-Roche).

## Supplementary References:

- 1 Dimple, C. *et al.* Role of PELP1/MNAR signaling in ovarian tumorigenesis. *Cancer Res* **68**, 4902-4909, doi:10.1158/0008-5472.CAN-07-5698 (2008).
- 2 Nair, S. S. *et al.* PELP1 is a reader of histone H3 methylation that facilitates oestrogen receptor-alpha target gene activation by regulating lysine demethylase 1 specificity. *EMBO Rep* **11**, 438-444, doi:embor201062 [pii] 10.1038/embor.2010.62 (2010).
- 3 Dobin, A. *et al.* STAR: ultrafast universal RNA-seq aligner. *Bioinformatics* **29**, 15-21, doi:10.1093/bioinformatics/bts635 (2013).
- 4 Habegger, L. *et al.* RSEQtools: a modular framework to analyze RNA-Seq data using compact, anonymized data summaries. *Bioinformatics* **27**, 281-283, doi:10.1093/bioinformatics/btq643 (2011).
- 5 Giannopoulou, E. G. & Elemento, O. An integrated ChIP-seq analysis platform with customizable workflows. *BMC bioinformatics* **12**, 277, doi:10.1186/1471-2105-12-277 (2011).
- 6 Pruitt, K. D., Tatusova, T., Brown, G. R. & Maglott, D. R. NCBI Reference Sequences (RefSeq): current status, new features and genome annotation policy. *Nucleic Acids Res* **40**, D130-135, doi:10.1093/nar/gkr1079 (2012).
- 7 Harrow, J. *et al.* GENCODE: The reference human genome annotation for The ENCODE Project. *Genome Res* **22**, 1760-1774, doi:10.1101/gr.135350.111 (2012).
- 8 Amaral, P. P., Clark, M. B., Gascoigne, D. K., Dinger, M. E. & Mattick, J. S. lncRNADB: a reference database for long noncoding RNAs. *Nucleic Acids Res* **39**, D146-151, doi:10.1093/nar/gkq1138 (2011).
- 9 Washietl, S., Hofacker, I. L. & Stadler, P. F. Fast and reliable prediction of noncoding RNAs. *Proc Natl Acad Sci U S A* **102**, 2454-2459, doi:10.1073/pnas.0409169102 (2005).
- 10 Rederstorff, M. *et al.* RNPomics: defining the ncRNA transcriptome by cDNA library generation from ribonucleo-protein particles. *Nucleic Acids Res* **38**, e113, doi:10.1093/nar/gkq057 (2010).
- 11 Sasaki, Y. T. *et al.* Identification and characterization of human non-coding RNAs with tissue-specific expression. *Biochem Biophys Res Commun* **357**, 991-996, doi:10.1016/j.bbrc.2007.04.034 (2007).
- 12 Quinlan, A. R. & Hall, I. M. BEDTools: a flexible suite of utilities for comparing genomic features. *Bioinformatics* **26**, 841-842, doi:10.1093/bioinformatics/btq033 (2010).
- 13 Ross-Innes, C. S. *et al.* Cooperative interaction between retinoic acid receptor-alpha and estrogen receptor in breast cancer. *Genes Dev* **24**, 171-182, doi:10.1101/gad.552910 (2010).
- 14 Yu, J. *et al.* An integrated network of androgen receptor, polycomb, and TMPRSS2-ERG gene fusions in prostate cancer progression. *Cancer cell* **17**, 443-454, doi:10.1016/j.ccr.2010.03.018 (2010).
- 15 Pflueger, D. *et al.* Discovery of non-ETS gene fusions in human prostate cancer using next-generation RNA sequencing. *Genome Res* **21**, 56-67, doi:10.1101/gr.110684.110 (2011).
- 16 Chakravarty, D. *et al.* Extranuclear functions of ER impact invasive migration and metastasis by breast cancer cells. *Cancer Res* **70**, 4092-4101, doi:10.1158/0008-5472.CAN-09-3834 (2010).

- 17 Benjamini, Y., and Yosef Hochberg. Controlling the False Discovery Rate: A Practical and Powerful Approach to Multiple Testing. *Journal of the Royal Statistical Society. Series B (Methodological)* **57**, 289–300 (1995).
- 18 Parkhomchuk, D. *et al.* Transcriptome analysis by strand-specific sequencing of complementary DNA. *Nucleic Acids Res* **37**, e123, doi:10.1093/nar/gkp596 (2009).